Donald Geon [illegible] LEC [illegible] TEX

1

LECTURE 2

COSMIC RAY PROTONS AND PHOTONS

I. PROTONS

IN THE 1920'S MILLIKAN ADVOCATED THAT COSMIC RAYS WERE PHOTONS, FROM NUCLEAR REACTIONS IN STARS. BY THE LATE 1930'S DETECTORS AT HIGH ALTITUDES SHOWED A CLEAR EAST-WEST ASYMMETRY OF ARRIVAL DIRECTION, INDICATING THE PRIMARY PARTICLES ARE CHARGED.

MEASUREMENTS IN STACKS OF NUCLEAR EMULSIONS FLOWN IN BALLOONS IN THE 1940'S AND '50'S SHOWED THAT THE PRIMARIES ARE LARGELY PROTONS. THE ENERGY SPECTRA WERE MEASURED UP TO ABOUT 100 GeV, VIA THE ENERGY LOSS, dE/dx.

FIG 15

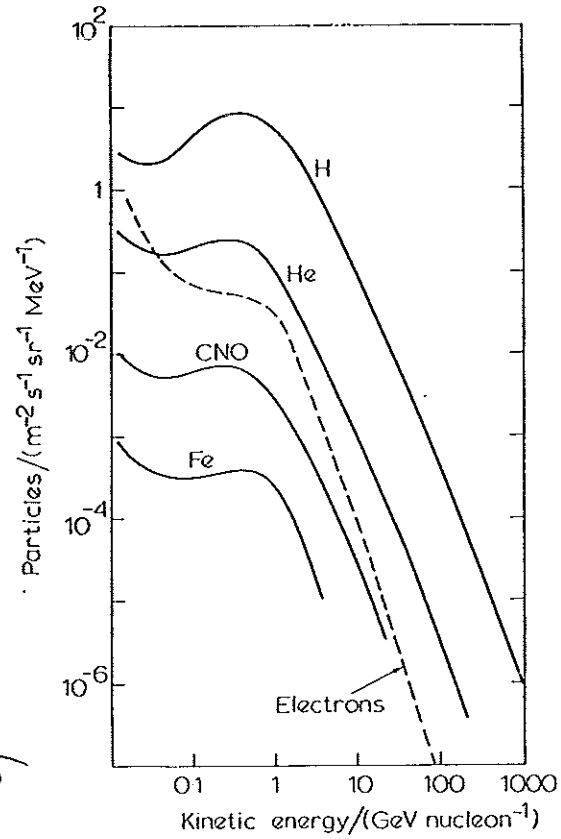

Fig. 22. Energy spectra per nucleon of primaries over the range for which these particles can be directly detected in balloon or satellite-carried equipment. The curve marked 'CNO' refers to almost equal amounts of carbon and oxygen with a small admixture of nitrogen; that marked 'Fe' does not distinguish between iron and its immediate neighbours. The lower ends of these spectra (energy per nucleon less than 10 GeV) are strongly modified by solar modulation: the amount of depression of intensity here varies through the solar cycle, and at the lowest energies some particles originating at the sun are also present. Outside the influence of the solar system the spectrum above 10 GeV nucleon^{-1} would probably continue smoothly to lower energies (see fig. 25). The broken line refers to the electron spectrum, and for this curve the units will be GeV and m^{-2} s^{-1} sr^{-1} MeV^{-1}.

IN THE 1950'S AND 1960'S EXTENSIVE ARRAYS OF DETECTORS AT GROUND LEVEL SAMPLED THE TRANSVERSE SHAPE OF PROTON-INDUCED AIR SHOWERS. THE PRIMARY ENERGY IS INFERRED AS A ROUGHLY LINEAR FUNCTION OF THE SHOWER SIZE. THE DETECTORS ARE TYPICALLY PLASTIC SCINTILLATORS, WHICH COUNT THE NUMBER OF MINIMUM IONIZING PARTICLES. FOR REASONS OF COST, WATER ČERENKOV DETECTORS ARE ALSO USED.

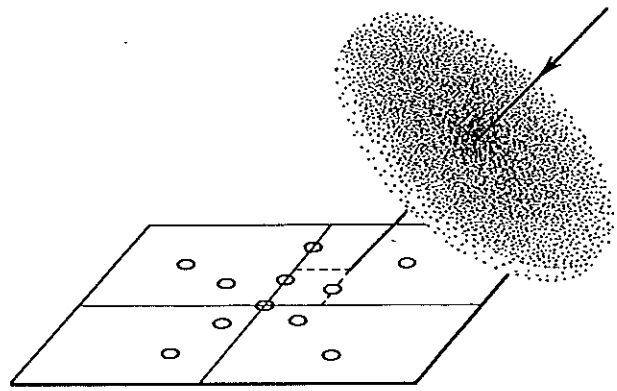

Fig. 12-4 Shower disk approaching detectors (represented by circles on a horizontal plane).

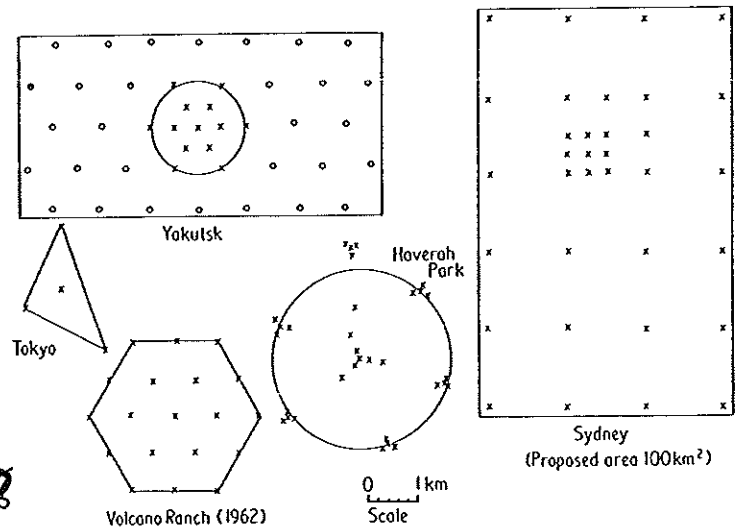

Figure 1. Sketch maps of large shower arrays. Detector systems which are, or have been, in use are shown ×; planned extensions to the arrays are shown thus O.

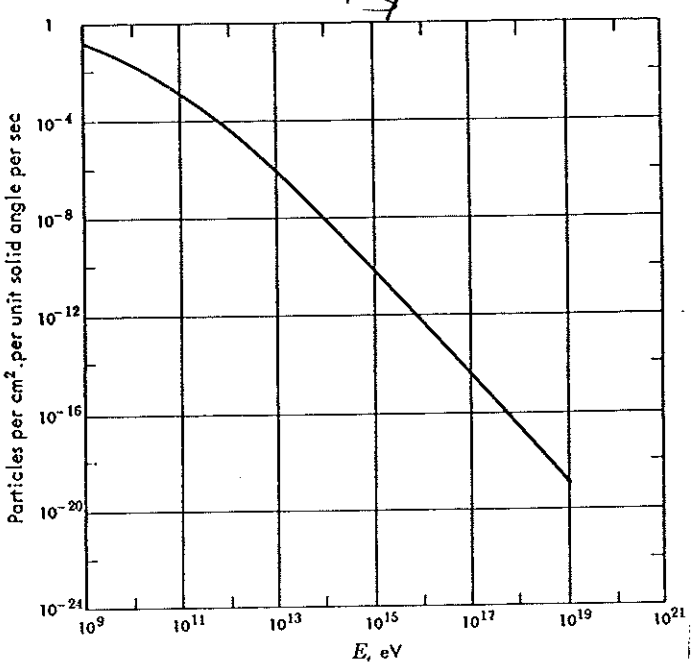

Fig. 11-6 Energy spectrum of primary cosmic rays. Plotted on the horizontal axis is the energy E of cosmic-ray particles, in electron volts. Plotted on the vertical axis is the directional intensity (see Fig. 11-5) for particles of energy *greater* than E striking the atmosphere above the geomagnetic poles (where the effect of the earth's magnetic field is negligible). The portion of the curve between 10^9 and 10^{11} eV was obtained from balloon measurements of the geomagnetic-latitude effect. Observations with nuclear emulsions exposed at balloon altitudes have provided some data in the energy region between 10^{11} and 10^{13} eV (the particle energy being estimated from the characteristics of their nuclear interactions). All data beyond 10^{16} eV come from experiments on air showers (Chap. 12). Note that the energy varies from about 1 BeV (10^9 eV) to about 10 billion BeV (10^{19} eV). Actually, the largest energy recorded, as of August, 1962, was 6×10^{19} eV (equal to the energy required to lift a mass of about one kilogram to a height of one meter). Note also the enormous range of intensity, which varies from about 0.15 particle per square centimeter per unit solid angle per second at 10^9 eV to a value about 10^{18} times smaller at 10^{19} eV. Since it can be shown that the total flux of particles from all directions above the horizon is π times the directional intensity, we find that a detector of 2 cm² at the top of the atmosphere will record about one primary particle per second and that the whole atmosphere (about 10^{16} cm² in area) will receive, every second, about two or three particles with energies above 10^{19} eV.

THROUGHOUT THE MEASURED ENERGY RANGE THE PRIMARY PROTONS APPEAR ISOTROPICALLY DISTRIBUTED. LITTLE HAS BEEN LEARNED FROM THESE DATA AS TO THE ASTROPHYSICAL SOURCE OF THE PROTONS.

II. PHOTONS

THE RESURGENCE OF ASTROPARTICLE PHYSICS IN THE LAST 20 YEARS IS ASSOCIATED WITH DETECTION OF γ-RAYS FROM POINT SOURCES. PERHAPS THIS VINDICATES THE EARLIER PREJUDICE OF MILLIKAN THAT COSMIC RAY PHYSICS SHOULD BE ABOUT EXACTLY THIS.

FIRST WE PRESENT AN INTERLUDE OF COLOR SLIDES, DISTRIBUTED BY THE ASTRONOMICAL SOCIETY OF THE PACIFIC, WHICH HELPS SET THE CONTEXT OF γ-RAY ASTROPHYSICS. 24

1. THE SKY AT 73-CM WAVELENGTH (408 MHZ). THIS RADIO EMISSION IS LARGELY DUE TO SYNCHROTRON RADIATION OF ELECTRONS
2. THE 21-CM SKY (1420 MHZ). HYDROGEN HYPERFINE LINE.
3. THE 3°K BACKGROUND (24.5 GHZ). THE ASYMMETRY OF 0.003°K IMPLIES MOTION OF THE EARTH BY ~ 600 KM/S WITH RESPECT TO THE BACKGROUND.
4. THE CO LINE AT 5 MM (115 GHZ)
5. THE INFRARED SKY

   RED = 100 μM = HYDROGEN DUST CLOUDS

   GREEN = 60 μM

   BLUE = 12 μM = HYDROCARBON DUST CLOUDS

6. 245,889 INFRARED POINT SOURCES

BLUE = STARS

YELLOW-GREEN = GALAXIES

7. THE VISIBLE SKY

8. SOFT X-RAY SKY, 60 Å (200 eV) AS SEEN VIA SOUNDING ROCKETS. 6 POINT SOURCES + DIFFUSE BACKGROUND.

9. 842 X-RAY SOURCES, 1-10 KeV, AS SEEN BY THE HEAO A-1 SATELLITE.

10. 2×10^5 γ-RAYS, 1-10 MeV, OBSERVED WITH THE COS-B SATELLITE. 25 POINT SOURCES + DIFFUSE BACKGROUND.

WE NOW REVIEW THE CONTRIBUTIONS OF SINGLE-PARTICLE DETECTORS TO γ-RAY ASTRONOMY, COVERING THE RANGE FROM 1 TO $\sim 10^{18}$ eV.

A. OPTICAL DETECTORS

THE CLASSIC OPTICAL DETECTION MEDIUM, FILM, REQUIRES ~100 PHOTONS TO STRIKE A 1-μm GRAIN BEFORE THE LATTER IS 'EXPOSED'. HENCE FILM IS NOT REALLY A SINGLE-PHOTON DETECTOR, ALTHOUGH WE MAY SAY THAT ITS QUANTUM EFFICIENCY IS ~1%.

PHOTOMULTIPLIERS, AVAILABLE SINCE ~1940, CAN DETECT SINGLE PHOTONS, BUT ARE ESSENTIALLY 1-PIXEL DEVICES, AND HAVE PLAYED LITTLE ROLE IN OPTICAL ASTRONOMY.

FILM HAS BEEN ALMOST UNIVERSALLY REPLACED AS THE RECORDING DEVICE IN OPTICAL TELESCOPES BY CCD'S (CHARGED-COUPLED DEVICE). FOR A TYPICAL APPLICATION, THE PALOMAR TELESCOPE, SEE GUNN ET AL., PUB. ASTRO. SOC. PAC. 99 518 (87). 195

OPERATION OF A CCD

[FROM DAMERELL, RAL-86-077]

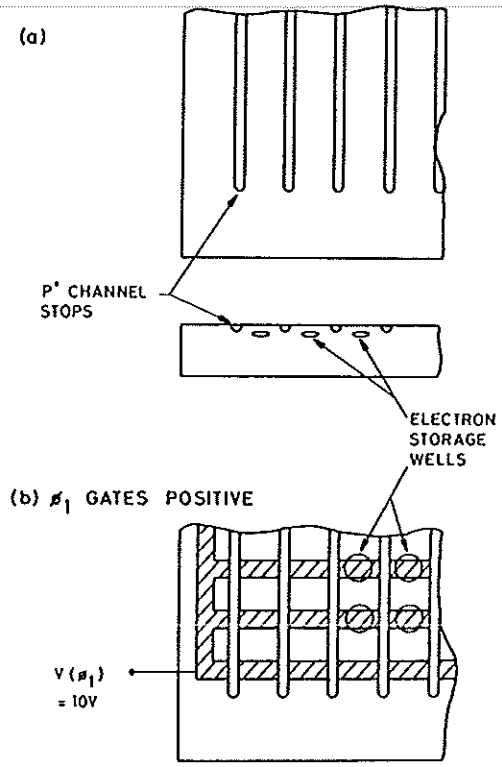

Figure 34 Establishing the potential well structure:
(a) Channel stops create potential barriers running vertically on the device.
(b) Gates create horizontal potential barriers. The combined result is a matrix of localised wells, each of which constitutes a pixel.

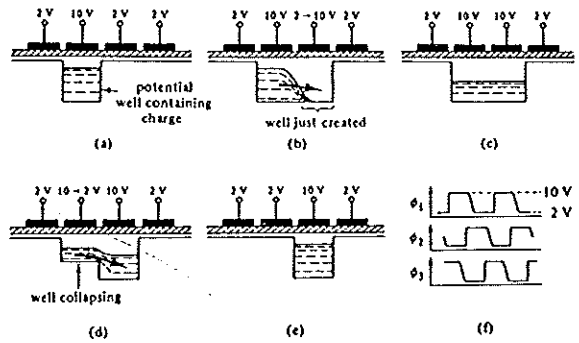

Figure 35 From Reference 32.
(a) to (e) Movement of potential well and associated charge packet by clocking of gate electrode voltages.
(f) Clocking waveforms for a 3-phase CCD.

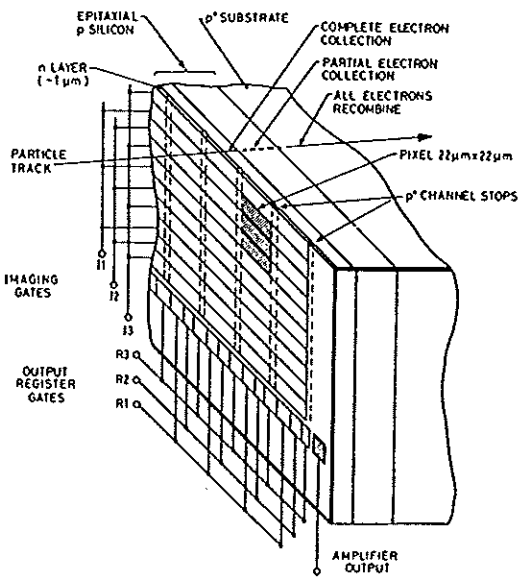

Figure 36 One corner of a CCD enlarged to show details of the pixel (storage element) structure.

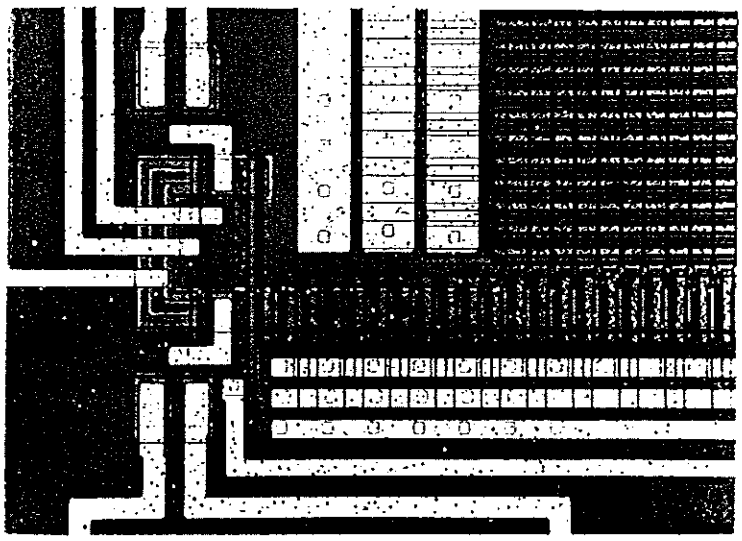

Figure 37 Courtesy of GEC, England. Photograph of one corner of a CCD showing the pixels of the imaging area (upper right quadrant), readout register (running along the bottom of the imaging area and extending 10 pixels to the left of it) and output FET (below and to the left of the readout register). The light coloured structures are aluminium tracks which carry the drive pulses to the gates, connections to the FETs, etc. The 3 broad bus-lines running vertically carry the Iϕ voltages, and the 3 narrow lines running horizontally carry the Rϕ voltages.

THE CCD HAS MANY DESIRABLE FEATURES

- QUANTUM EFFICIENCY ~50% IN VISIBLE (SILICON)
- PIXEL SIZE ~ 25 x 25 μm
- PIXEL ARRAY ~ 500 x 500 (AS FOR TELEVISION)
- DYNAMIC RANGE UP TO 10^5
- READOUT IN 1/30 SEC WITH NOISE OF A FEW x 100 $e^{'s}$/PIXEL.
- READOUT IN 60 SEC WITH < 5 $e^{'s}$/PIXEL NOISE (WHEN CCD COOLED TO 100°K TO SUPPRESS SHOT NOISE).

CCD'S CAN BE COATED WITH PHOSPHORS FOR UV SENSITIVITY, AND ARE DIRECTLY SENSITIVE TO KeV X-RAYS, WHICH ARE ABSORBED VIA THE PHOTOELECTRIC EFFECT IN THE 20-μm ACTIVE LAYER OF DEPLETED SILICON.

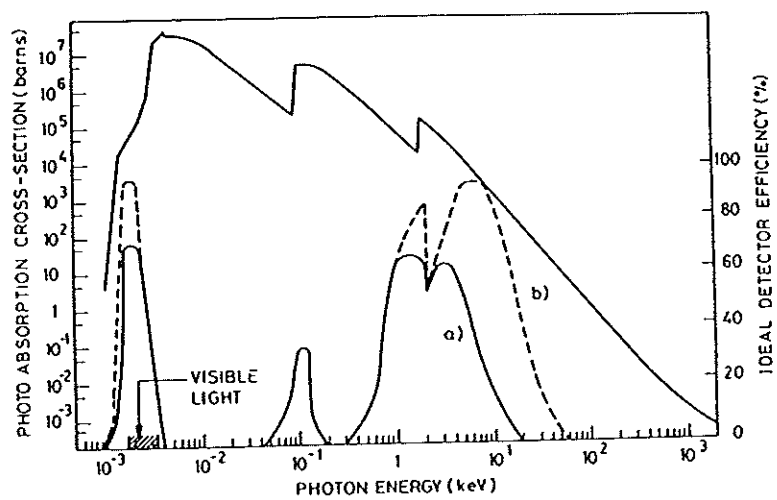

Figure 9 Experimental photoabsorption cross-section for silicon, indicating the energy ranges of use for the detection of real photons.

AT BEST, ~20 PHOTOELECTRONS/PIXEL ARE REQUIRED FOR A CLEAR SIGNAL ABOVE NOISE; SINGLE PHOTON SENSITIVITY HAS NOT BEEN ACHIEVED. HOWEVER THIS IS ATTAINABLE IF THE CCD IS COMBINED WITH A MICROCHANNEL PLATE (MCP). THIS DEVICE CAN GIVE A GAIN OF > 10^3 WHILE MAINTAINING 50-μm RESOLUTION.

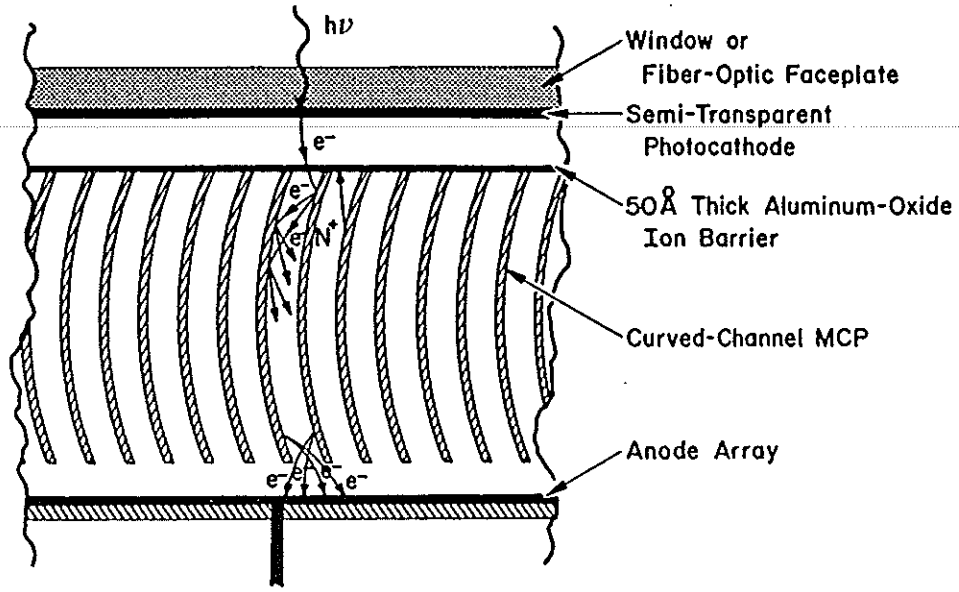

27

FIG. 13—Schematic of a curved-channel MCP array detector with a proximity-focused semitransparent photocathode (from Timothy and Bybee 1983).

AN IMPORTANT APPLICATION OF AN OPTICAL CCD TO ASTROPARTICLE PHYSICS IS THE WORK OF LOH & SPILLAR, AP. J. 307, 61 (1986). (28)

THEY MEASURE THE SPECTRA OF DISTANT GALAXIES, PLACING A SERIES OF 6 FILTERS IN FRONT OF A CCD AT THE FOCUS OF A 2.3-M TELESCOPE. FROM A SAMPLE OF 1000 GALAXIES THEY INFER THE DISTRIBUTION OF THEIR REDSHIFTS (BY COMPARING AGAINST SPECTRA OF GALAXIES WITH SMALL REDSHIFT). THEY THEN FIT THE REDSHIFT DISTRIBUTION TO A HYPOTHESIS AS TO THE MASS DENSITY OF THE UNIVERSE. A CLOSED UNIVERSE IMPLIES FEWER GALAXIES WITH LARGE REDSHIFTS $= z = \frac{\lambda_0 - \lambda_{OBS}}{\lambda_{OBS}}$.

THE DATA FAVOR (WEAKLY) A CLOSED UNIVERSE: $\Omega = \frac{\rho_{OBS}}{\rho_{CRITICAL}} = 0.9^{+0.7}_{-0.5}$

IT IS CLAIMED THAT $\Omega_{BARYON} < 0.2$, SO THERE MUST BE DARK MATTER ON THE LARGEST SCALE.

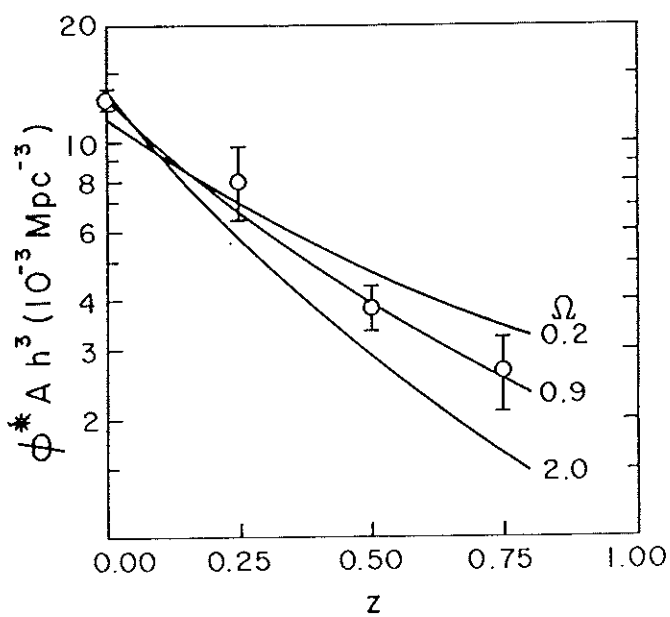

B. X-RAY DETECTION

1. PROPORTIONAL COUNTERS

X-RAYS ARE LARGELY ABSORBED IN THE ATOMSPHERE AT HEIGHTS OF LESS THAN 100 KM. DETECTORS ON BALLOON FLIGHTS IN THE 1950'S DID NOT HAVE SUFFICIENT SENSITIVITY TO DETECT THE ATTENUATED FLUX AT ACCESSIBLE ALTITUDES. NOTABLE SUCCESS CAME WITH A SIMPLE DETECTOR FLOWN IN AN AEROBEE ROCKET [GIACCONI ET AL, P.R.L. 9, 439 (1962)]

A SIMPLE AND LIGHTWEIGHT X-RAY DETECTOR IS THE GAS-FILLED PROPORTIONAL COUNTER. THE DESIGN DATES TO THE ERA OF RUTHERFORD.

THE PRINCIPAL INNOVATION OF GIACCONI'S DETECTOR WAS A THIN MICA WINDOW ($1.4\ mg/cm^2$) WHICH ALLOWED GOOD DETECTION EFFICIENCY FOR 2-10 KeV X-RAYS.

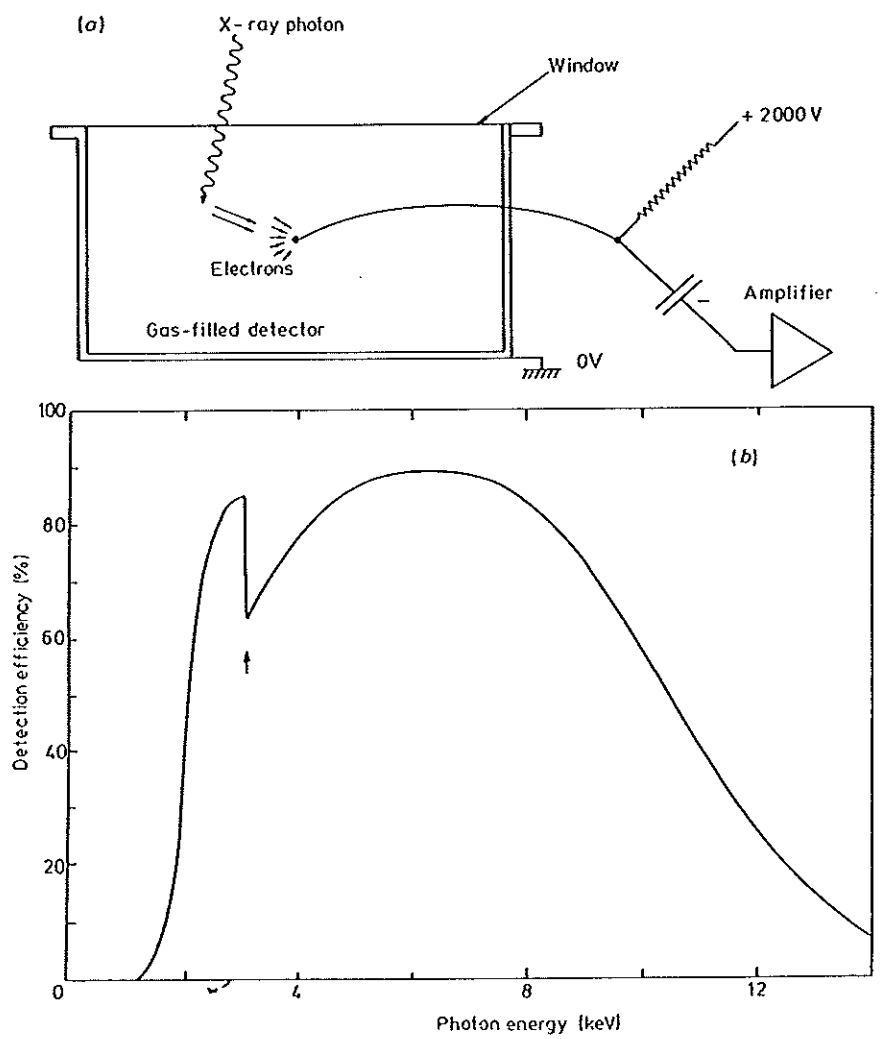

Figure 2.2. (*a*) Proportional-counter detector operation. (*b*) Photon detection efficiency of a typical argon-filled detector. The feature at about 3 keV is the K-edge of argon.

FIG 23 REF 30

THE DETECTOR AS MOUNTED HAD A FIELD OF VIEW OF ± 30°. THE ROCKET ROTATED ABOUT ITS AXIS, AND THE NUMBER OF X-RAY COUNTS WAS RECORDED IN INTERVALS CORRESPONDING TO 1° OF ROTATION.

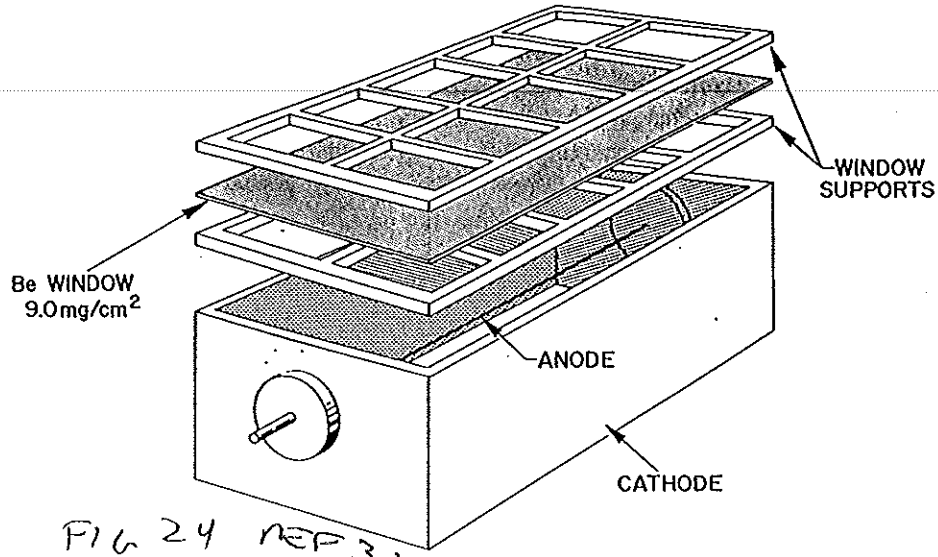

FIG 24 REF 31

Fig. 2.10. Schematic layout of a thin window gas proportional counter. The Be window is cemented between a supporting 'sandwich' which in turn is hermetically sealed to the cathode to preserve the gas integrity. The anode is usually kept under tension by a spring. The charge sensitive preamp and high voltage power supply are ideally mounted as close as possible to the anode feed-through.

THE FIRST ROCKET FLIGHT WAS FORTUNATE IN REVEALING A STRONG, LOCALIZED X-RAY SOURCE, SCORPIO X-1.

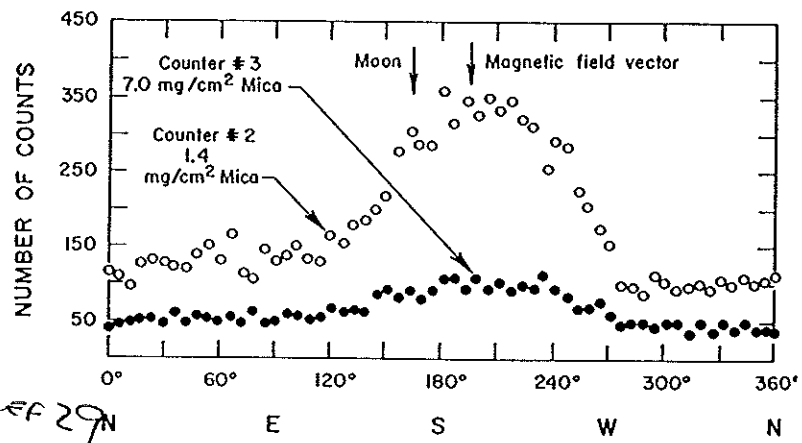

FIG 25, REF 29

Azimuthal distributions of recorded counts from Geiger counters flown during June, 1962. (R. Giacconi et al., *Physical Review Letters* 9 (1962), 439)

LATER VARIATIONS ON THE PROPORTIONAL COUNTER INCLUDE COLLIMATORS OVER THE COUNTER WINDOW TO LIMIT THE FIELD OF VIEW TO ~ 1° × 5°.

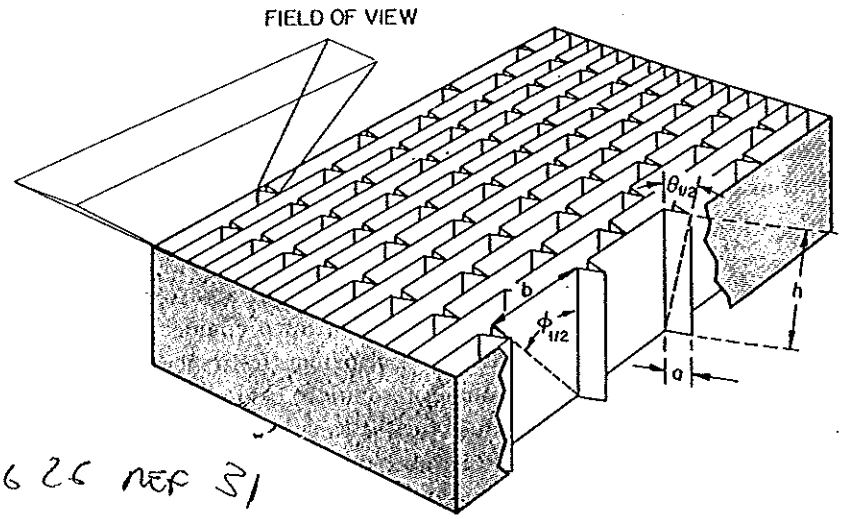

FIG 26 REF 31

Fig. 2.16. A slat collimator, comprised of rectangular tubes of height h and cross section $a \times b$. X-rays which strike the tubes cannot reach the detector. The response pattern within the field of view has a triangular shape in each of the two orthogonal directions. The half-transmission angles are determined simply by the geometry: $\tan\theta_{1/2} = a/h$; $\tan\phi_{1/2} = b/h$.

A STRIKING MEASUREMENT WITH PROPORTIONAL COUNTERS WAS THE IDENTIFICATION OF SOME X-RAY SOURCES AS BINARY PULSARS, AS REVEALED BY LONG- AND SHORT-TERM PERIODICITIES.

THE INTENSE X-RAY RADIATION OF SUCH SOURCES LENDS CONFIRMATION TO THE HYPOTHESIS THAT THEY ARE NEUTRON STARS.

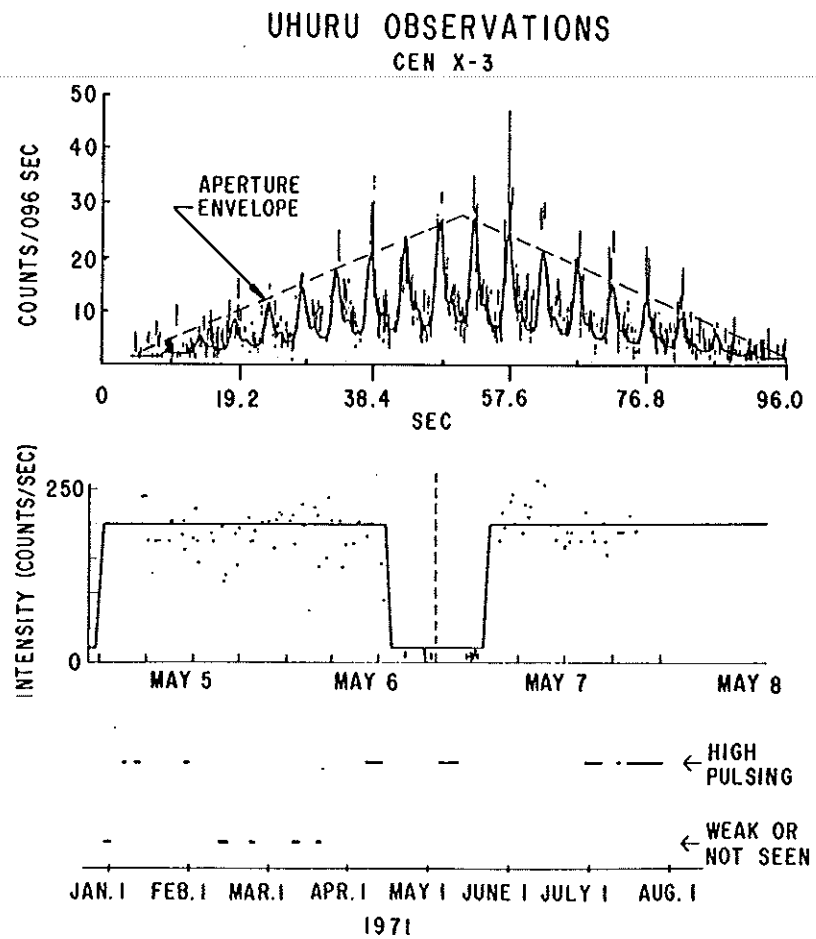

Figure 2 Time variations observed on three different scales from the binary source Cen X-3. *Upper curve*, the 4.8^{+}-sec pulses during a single UHURU scan; *middle panel*, the 2.067-day variation associated with the binary eclipse; *lower panel*, the long-term quasi-random "on" and "off" states. (Adapted from Schreier et al 1972.)

FIG 2, REF 32

A RECENT APPLICATION IS BY DOTANI ET AL (33), NATURE 330, 230 (1987) WHO REPORT AN X-RAY SPECTRUM FROM SN 1987 A, TAKEN WITH DETECTORS ABOARD THE SATELLITE GINGA. THE CHARGE COLLECTED IN A PROPORTIONAL COUNTER IS, OF COURSE, PROPORTIONAL TO THE ENERGY DEPOSITED, PROVIDING A MEASURE OF THE X-RAY ENERGIES.

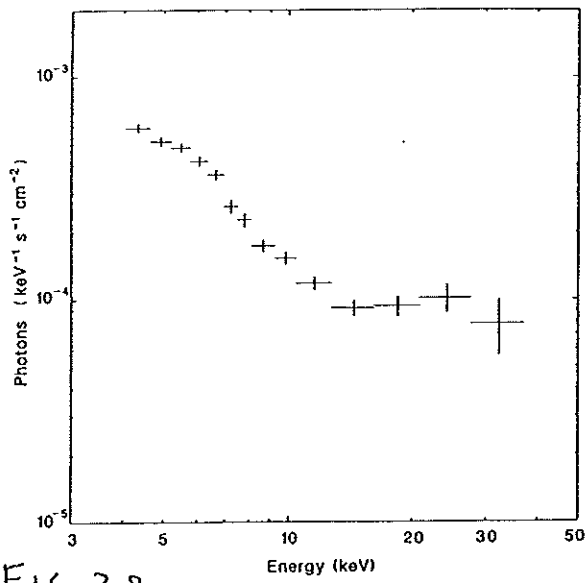

FIG 28 REF 33

Fig. 4 Photon number spectrum of the hard source obtained from pointing observations on 3 September, corrected for the detection efficiency. The detection efficiency as a function of X-ray energy was calibrated before launch and after (using the Crab nebula). The iron line intensity for the spectral model used was $(1.3 \pm 0.3) \times 10^{-4}$ photons cm^{-2} s^{-1}.

ANOTHER SIGNIFICANT VARIATION OF THE BASIC PROPORTIONAL COUNTER IS THE CODED-MASK IMAGING SPECTROMETER. IN THIS A GRID MASK OF ABOUT 50% OVERALL TRANSMISSION IS PLACED SOME DISTANCE IN FRONT OF THE COUNTER. THE SHADOW CAST ON THE DETECTOR (BY MANY X-RAYS FROM A POINT SOURCE) IS A COMPLICATED FUNCTION OF THE SOURCE ANGLE, WHICH IS TRANSFORMED BY A COMPUTER INTO AN ANGULAR MEASUREMENT. A WELL-DESIGNED MASK CAN YIELD ANGULAR RESOLUTION ~ 1/# OF PIXELS ON MASK. OF COURSE, THE DETECTOR MUST HAVE PIXEL SIZES SIMILAR TO THOSE OF THE MASK.

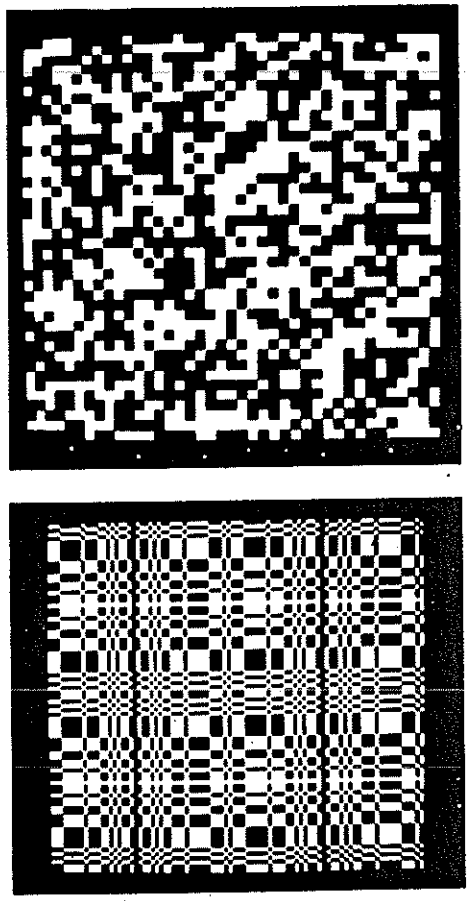

Two different coded-aperture patterns, each of which is about 50 percent transmitting. *Top:* A 40-by-40 element random pinhole array of the type designed by Robert Dicke. *Bottom:* A 43-by-41 element uniformly redundant array. Courtesy Harrison H. Barrett, Edward Fenimore, and the author.

FIG 29 REF 34

A RECENT APPLICATION IS BY SUNYAEV ET AL, NATURE 330, 227 (1987) WHO RESOLVE SN1987A FROM NEARBY LMC X-1 AND PSR 0540-693, WITH ACCURACY OF 2 ARC MINUTES. THEIR DETECTOR IS A XENON-FILLED PROPORTIONAL COUNTER WITH SENSITIVITY IN THE 2-30 KeV RANGE.

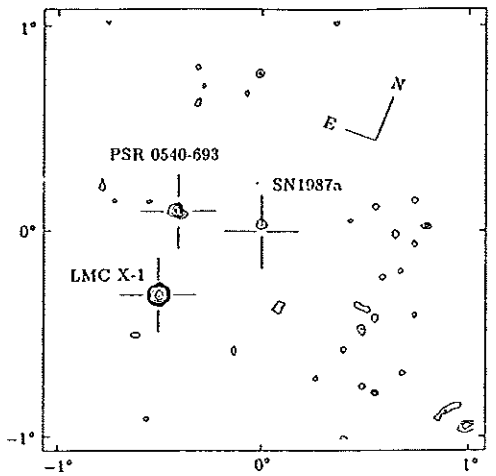

Fig. 3 Contour map of the 2° square region of the image in Fig. 2 surrounding SN1987A. Axes show offsets from the position of the supernova. Apart from LMC X-1 and 0540-693, the levels seen are consistent with the expected noise level. Contours are at 3, 4, 5, 6, 7, 8, 10, 20, 40 and 60×10^{-1} uncorrected counts per second.

FIG 30 REF 35

2. High-Angular-Resolution Detectors

To obtain angular resolution significantly better than 1′ requires a focusing optical system. These can be made with grazing-incidence mirrors for X-rays of ~0.1–1 keV, or with Bragg-scattering crystal mirrors for X-rays of ~1–10 keV.

The grazing-incidence mirror system was implemented on a large scale for the HEAO-2 (Einstein) satellite, launched in 1978. The accuracy obtained was ~ 1″, comparable to an optical telescope. This allowed clear confirmation of the X-ray sources with radio pulsars.

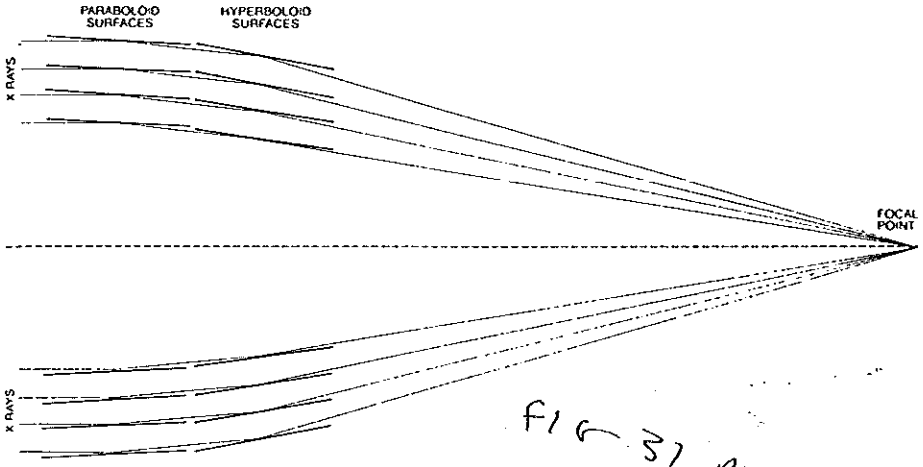

A schematic of a grazing-incidence telescope.

FIG 31 REF 36

The high resolution also permits detailed mapping of the X-ray emission of gas surrounding galaxies. The inferred density of gas + stars accounts for only 10% of the mass needed to explain the galactic dynamics: the dark matter problem on another scale!

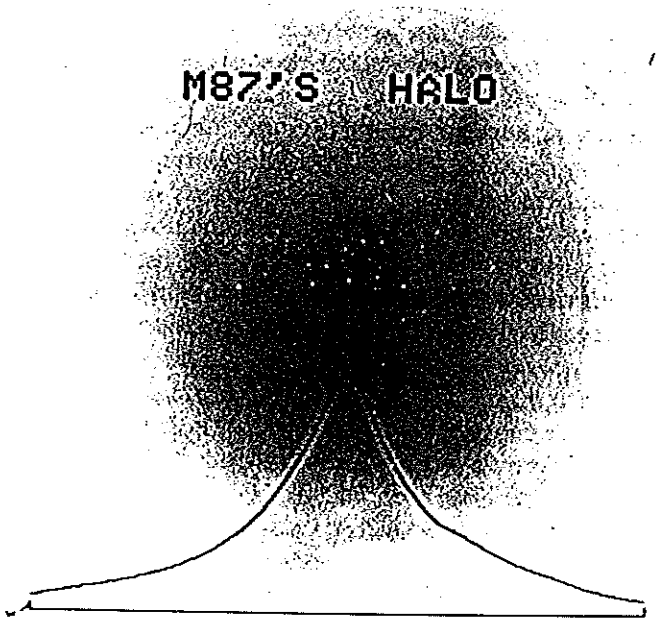

An x-ray image of the extended halo of the giant elliptical galaxy M87. (W. Forman and C. Jones, Harvard-Smithsonian Center for Astrophysics)

FIG 32 REF 36

3. HIGH-ENERGY-RESOLUTION DEVICES

THE BEST ENERGY RESOLUTION FOR X-RAYS IN A COMPACT DETECTOR IS OBTAINED WITH A Ge(Li) TOTAL ABSORPTION COUNTER. THIS IS A SOLID-STATE IONIZATION CHAMBER, AND ACHIEVES ~150 eV RESOLUTION FOR 6 KeV X-RAYS. HOWEVER, IT MUST BE OPERATED A LIQUID-NITROGEN TEMPERATURE.

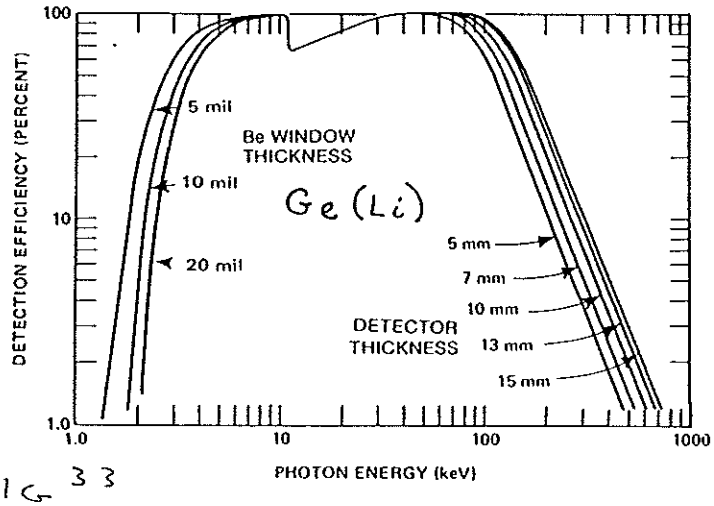

FIG 33

Efficiency vs Energy Curve as a Function of Be Window Thickness and Detector Thickness.

REF 37

THE BEST ROOM-TEMPERATURE DEVICE IS A NaI OR CsI SCINTILLATION DETECTOR. ALL 3 DETECTORS HAVE GOOD EFFICIENCY DOWN TO A FEW KeV, WITH EFFICIENCY FOR HIGH-ENERGY X-RAYS LIMITED BY DETECTOR THICKNESS. DEVICES FLOWN IN SATELLITES ARE USEFUL UP TO ~10 MeV.

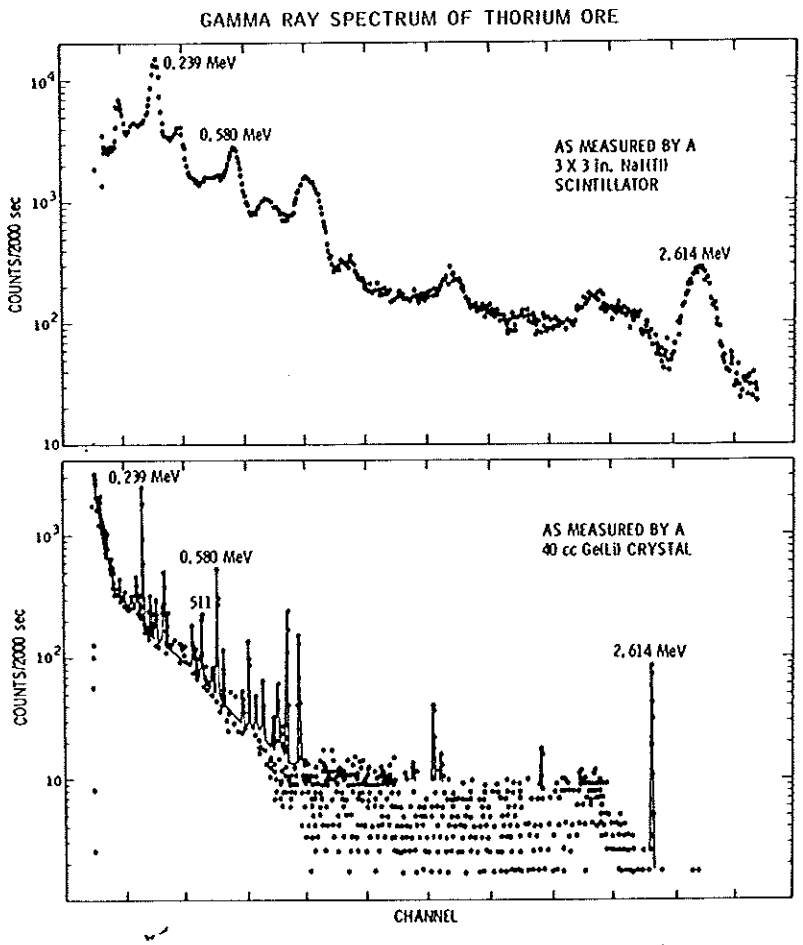

Comparison of Spectra as Measured by Ge(Li) and NaI(Tl) Crystals

Figure 17 Comparison of spectra measured by a NaI(Tl) crystal scintillator (*top*) and a Ge(Li) solid-state detector. The resolution available with the solid-state device is clearly far superior. The sensitivity of the (typically larger) scintillator is greater above ~1 MeV. (Courtesy Dr. A. E. Metzger.)

FIG 34 Ref 38

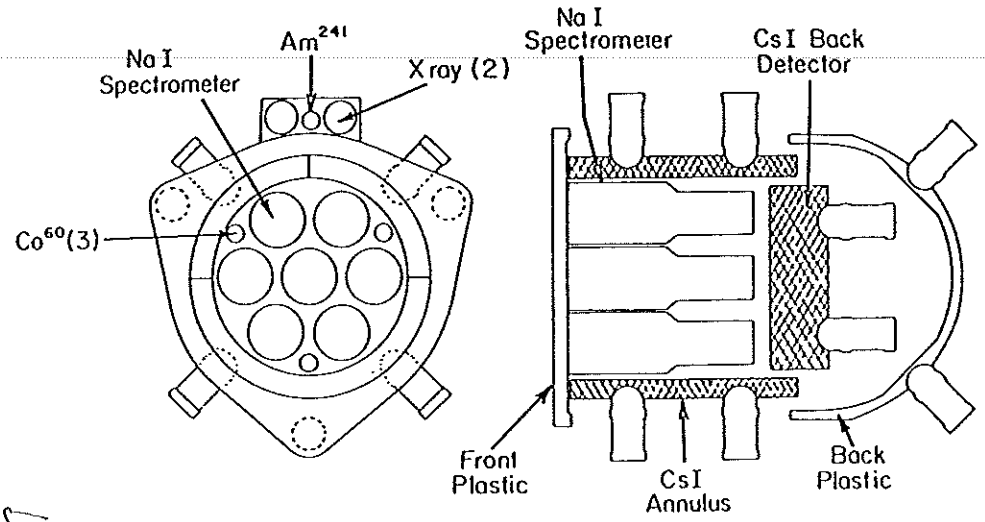

Fig 6 3r
Ref 39

Figure 11-16. Schematic drawing of the SMM γ-ray spectrometer experiment showing the major subsystem components in top and cross-sectional side views (reprinted with permission from David J. Forrest, Forrest et al., 1980).

A NaI/CsI DETECTOR HAS OBSERVED X-RAYS FROM SN 1987A [SUNYAEV ET AL, NATURE 330, 227 (1987)]. THE ANGULAR RESOLUTION OF THEIR DETECTOR IS DEFINED BY COLLIMATORS TO BE ABOUT 1.5°. WITHIN THAT RANGE ARE 2 OTHER X-RAY SOURCES, Fig 30 (p-11) LMC X-1, AND PSR 0540-693. THE X-RAY SIGNAL 180 DAYS AFTER SN 1987A WAS STILL ROUGHLY COMPATIBLE WITH THAT DUE TO THE PREVIOUSLY KNOWN SOURCES, BUT AT 210 DAYS THE SIGNAL HAD TRIPLED.

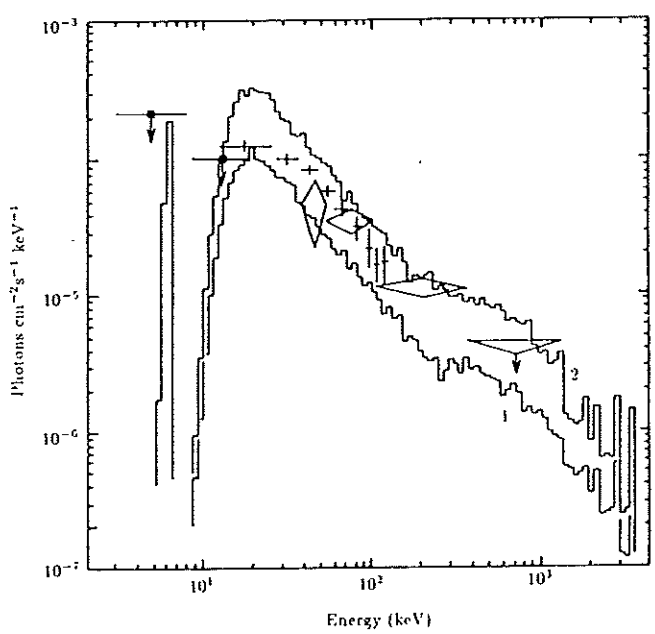

Fig. 1 Preliminary energy spectrum of the hard X-rays. Squares, 3σ upper limits from TTM; crosses, detections with HEXE (1σ error bars); diamonds, detections and 3σ upper limits obtained with Pulsar X-1. The histograms show the results of Monte Carlo simulations by Grebenev and Sunyaev[10], assuming 0.1 $M_\odot$ of ^{56}Co, an expanding envelope of 16 $M_\odot$ with metallicity 1/3 solar, and mean expansion velocity 4,150 km s^{-1}, 180 days (1) and 210 days (2) after the explosion. The histogram bins in the region of the Fe fluorescence line are 0.5 keV wide.

Fig 36
Ref 3r

UNTIL RECENTLY THE ONLY LINES OBSERVED IN X-RAY SPECTRA HAVE BEEN $^{26}Al \rightarrow 1.8$ MeV, AND $e^+e^- \rightarrow 511$ KeV.

MATZ ET AL, NATURE 331, 416 (1988) 40 REPORT EVIDENCE FOR X-RAYS FROM ^{56}Co DECAY IN SN1987A, USING THE DETECTOR OF THE SOLAR MAXIMUM MISSION (SMM, p. 14). THE AMOUNT OF ^{56}Co PRODUCED IN SN 1987 A HAS 70 TIMES THE MASS OF JUPITER!

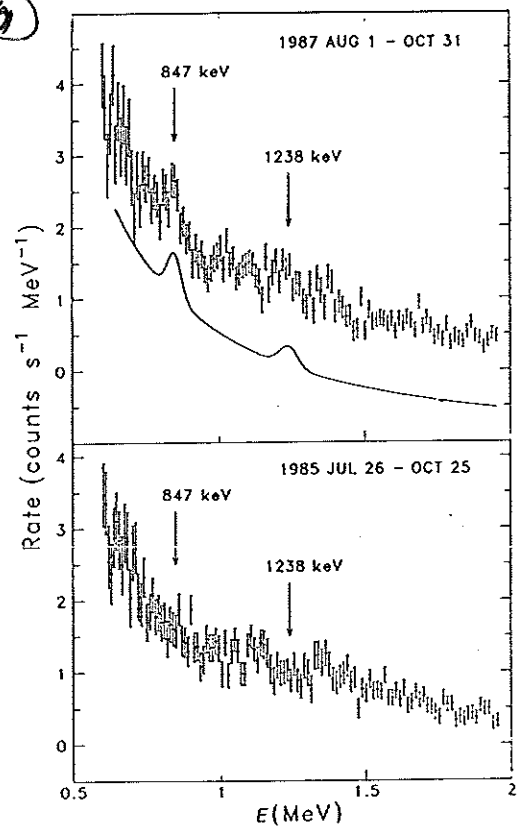

Fig. 2 The background-subtracted spectrum for SN1987A, accumulated from 1 August to 31 October 1987. The line profiles for the two ^{56}Co lines plus a power-law continuum are plotted as a solid line. Also shown is an equivalent spectrum accumulated in 1985. In both spectra residual features can be seen near 1.17 and 1.33 MeV due to imperfect subtraction of lines from the internal calibration source. Note also the residual atmospheric continuum in both spectra.

C. MEDIUM-ENERGY γ RAYS (30 MeV - 3 GeV)

γ RAYS OF ENERGY ABOVE 30 MeV INTERACT WITH MATTER PRIMARILY VIA PAIR PRODUCTION, AND SO INITIATE CASCADE SHOWERS. THESE SHOWERS DO NOT REACH GROUND LEVEL UNLESS THE γ ENERGY IS A FEW HUNDRED GeV. SPACE LIMITATIONS IN SATELLITES HAVE RESTRICTED SHOWER DETECTORS TO CONTAIN γ ENERGIES UP TO $\sim$ 5 GeV.

TYPICAL DETECTORS CONSIST OF A MULTIPLATE SHOWER CHAMBER, EXACTLY AS USED BY ROSSI IN THE 1930'S, BUT WITH ELECTRONIC READOUT. A ČERENKOV COUNTER CAN VERIFY THE SHOWER DIRECTION, AND THAT IT CONTAINS ELECTRONS. LEAKAGE OUT THE BOTTOM OF THE DETECTOR IS MONITORED WITH A FINAL ENERGY SAMPLING COUNTER.

THE RESOLUTION OF SUCH DETECTORS IS LIMITED, ESPECIALLY COMPARED TO THE SOLID-STATE DETECTORS WHICH OPERATE AT ONLY SLIGHTLY LOWER ENERGIES.

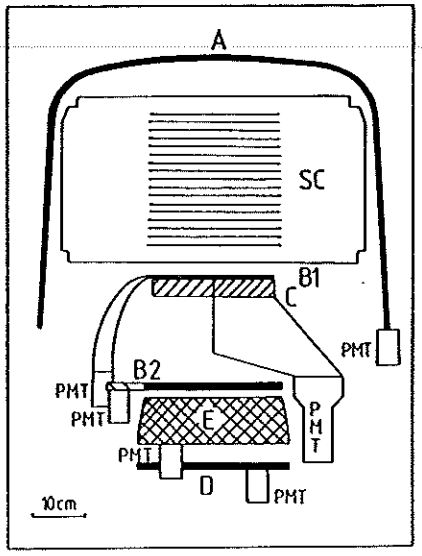

Fig 3b ref (1)

Figure 4.7. Sectional view of the COS B γ-ray detector (Bennett *et al.* 1976). A: anticoincidence counter; SC: spark chamber; B1, B2: scintillation counters, C: directional Cerenkov counter; E: energy calorimeter (caesium–iodide scintillator); D: scintillator to provide information on high energy events for which the absorption in the calorimeter is incomplete.

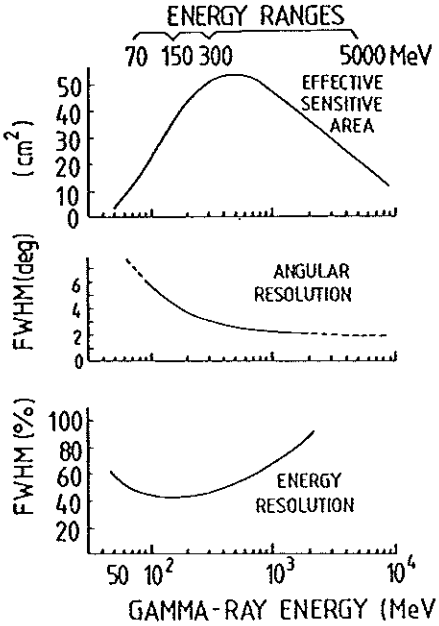

Fig 3a ref (4.1) 42

Figure 4.8. Characteristic parameters of the COS B experiment for γ-rays incident along the detector axis (Scarsi *et al.* 1981).

ENERGY SPECTRA (P. 17) COLLECTED WITH THE SHOWER CHAMBERS, WHEN COMBINED WITH THOSE FROM SOLID-STATE DETECTORS, SHOW A BEHAVIOR LIKE RATE $\sim 1/E_\gamma^2$, BOTH FOR DISCRETE SOURCES, AND FOR THE DIFFUSE γ-RAY BACKGROUND.

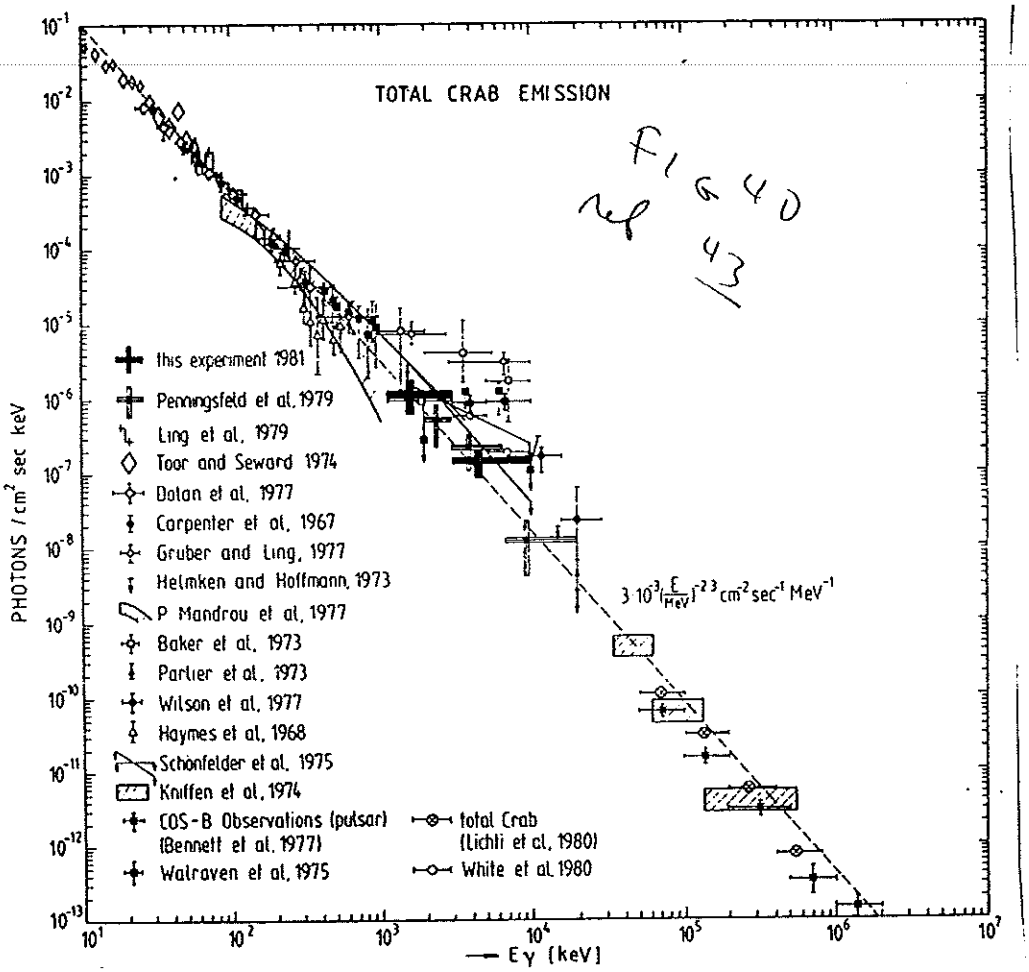

THE FIRST STEP OF A γ CASCADE IS PAIR PRODUCTION IN A NUCLEAR FIELD: $\gamma + A \rightarrow A' + e^+e^-$. THE PLANE OF THE $A' e^+e^-$ SYSTEM IS PREFERENTIALLY ALIGNED ALONG THE $\vec{E}$ VECTOR OF THE γ-RAY. RECENT MEASUREMENTS OF THE AZIMUTHAL DISTRIBUTION OF THIS PLANE FOR γ-RAYS FROM THE VELA X-1 PULSAR SHOW A 25% MODULATION, INDICATING STRONG LINEAR POLARIZATION [CARAVEO ET AL, AP. J. (1988)] = (44)

FIG 41 ref 44

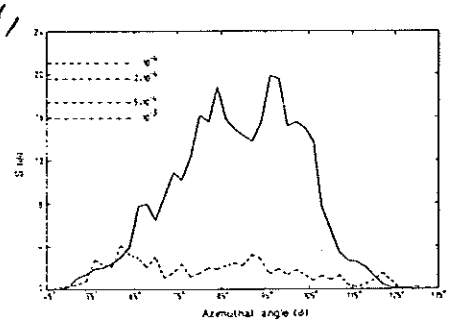

The azimuthal modulation of the plane containing the electron–positron pairs derived from 2,526 pulsed Vela γ-rays that materialize in the Cos-B spark chamber (solid curve). The dashed curve applies to 3,109 photons from the Cygnus region used as a comparison. S is the deviation function as defined in Caraveo *et al.* Overall chance occurrence probability levels are shown as derived from Monte-Carlo simulations.

THIS SUPPORTS THE HYPOTHESIS THAT THE MeV γ-RAYS ARE PRODUCED BY SYNCHROTRON RADIATION IN THE STRONG MAGNETIC FIELD SURROUNDING THE NEUTRON STAR.

ABOVE ~10 GeV THE γ SHOWERS ARE TOO LARGE FOR EFFECTIVE CONTAINMENT IN SATELLITE INSTRUMENTATION. THE FUTURE OF SPACE RESEARCH IN γ-RAYS LIES IN BETTER DETECTORS OVER THE ACCESSIBLE INFRARED TO X-RAY SPECTRA. THIS IS COSTLY. A RECENT DISCUSSION BY BROWN & GIACCONI [SCIENCE 238, 617 (1987)] SUGGESTS THAT FULL SUPPORT FOR SPACE ASTRONOMY WOULD REQUIRE ~ $700 M/YEAR IN THE USA ALONE.

D. γ RAYS ABOVE 100 GeV

THESE γ RAYS INITIATE SHOWERS WHICH MAY BE DETECTED AT GROUND LEVEL.

BETWEEN 100 GeV AND 1 TeV ENERGY ONE DETECTS THE ČERENKOV LIGHT FROM ELECTRONS IN THE SHOWER.

ABOVE 1 TeV THE ELECTRONS OF THE SHOWER MAY BE SAMPLED IN A DETECTOR ARRAY SIMILAR TO THOSE FOR PHOTON-INDUCED SHOWERS. Fig 41 of 46

THE EARLIEST ATMOSPHERIC ČERENKOV DETECTOR (P. 19) WAS BUILT IN A GARBAGE CAN ('DUSTBIN' IN BRITISH), AND MANY PRESENT DETECTORS LOOK RATHER SIMILAR. Fig 42

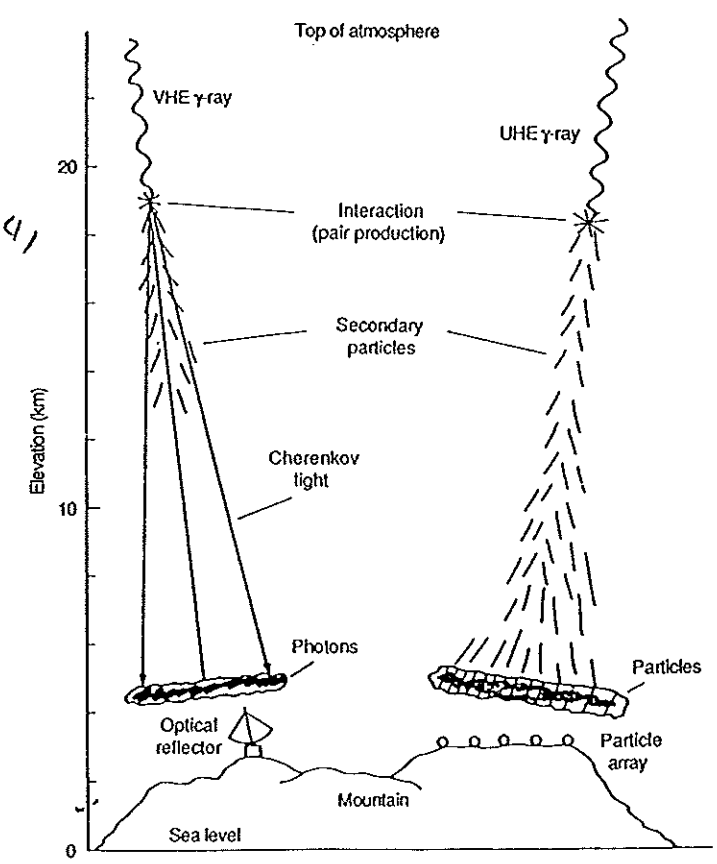

Fig. 1. Schematic view of two air showers created in the atmosphere. The VHE gamma ray is detected by the Cherenkov light emitted from the relativistic electrons and positrons of the shower. The higher energy UHE gamma ray creates numerous particle secondaries that penetrate to ground-based particle detector arrays.

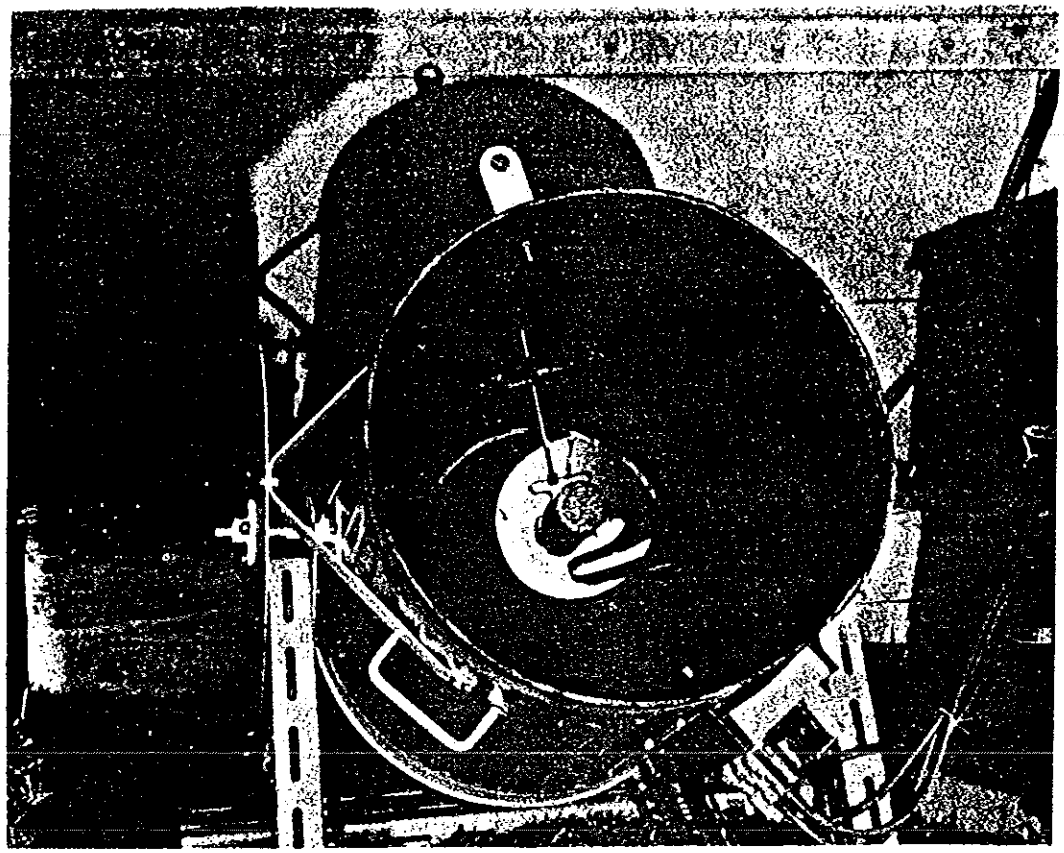

FIG 42 ref 47

FIGURE 1

The original Cherenkov light receiver built by Galbraith and Jelley, comprising a 25 cm. f/0.5 rear-silvered ex World War II signalling mirror, and a 50 mm EMI photomultiplier, mounted in a dustbin.

48

FIG 44 ref 48

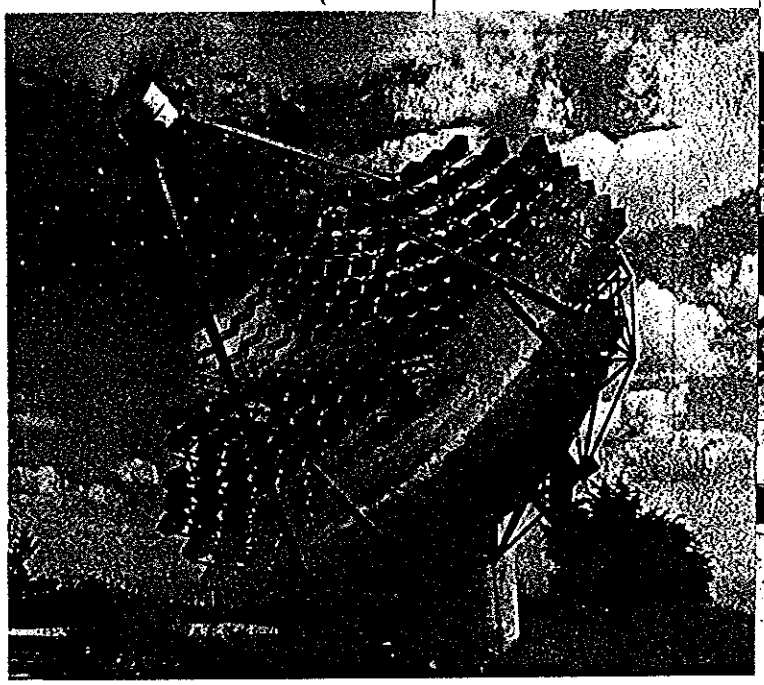

Figure 5.5. A picture of the 10 m reflecting night sky Cerenkov telescope of the Fred Lawrence Whipple Observatory at Mt. Hopkins, USA. (Smithsonian Institution – courtesy of Prof. T. C. Weekes.)

FIG 43 ref 48

Figure 5.6. The 18 parabolic mirror array to detect Cerenkov light produced by showers. The array was operated by the Tata Institute of Fundamental Research group at Ootacamund (Ooty), India. Two small mirrors were not used in the experiment. (Photograph by A. R. Apte.)

HIGH-ENERGY γ-RAY SIGNALS HAVE BEEN OBSERVED FROM THE BRIGHTEST BINARY X-RAY PULSARS. THE SIGNAL IS GENERALLY APPARENT AGAINST THE DIFFUSE BACKGROUND ONLY WHEN IT HAS A MODULATION AT SOME CHARACTERISTIC PERIOD OF THE BINARY SYSTEM. THE SHARPNESS OF THE MODULATIONS SUGGESTS THAT THE HIGHEST ENERGY γ RAYS ARE ASSOCIATED WITH AN ORIENTED FLOW OF MATTER FROM ONE MEMBER OF THE BINARY PAIR TO THE OTHER.

Fig 4 ref 46

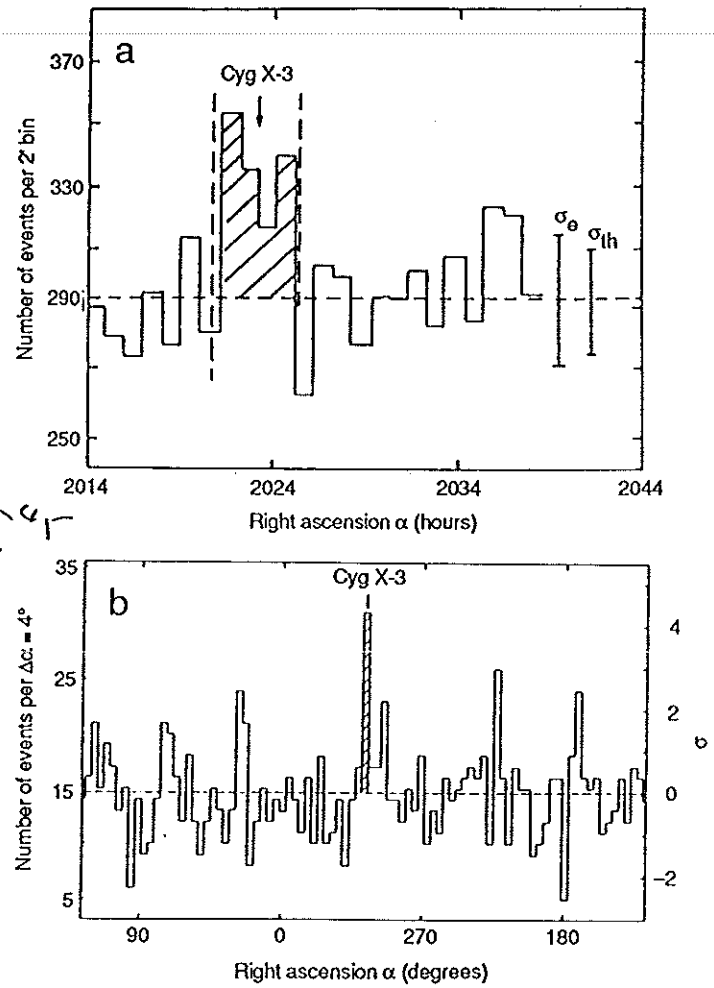

Fig. 2. First clear source detections at TeV and PeV energies. (a) Crimean Astrophysical Observatory observations in 1972 of Cygnus X-3 at energies of about 1 TeV (7). The standard error on the number of events in a bin has been derived in two ways: from counting statistics (σ_{th}) and from the experimentally observed fluctuations (σ_e). (b) University of Kiel observations of Cygnus X-3 from 1976–1980 at energies above 2 PeV (8).

Fig 46 ref 49

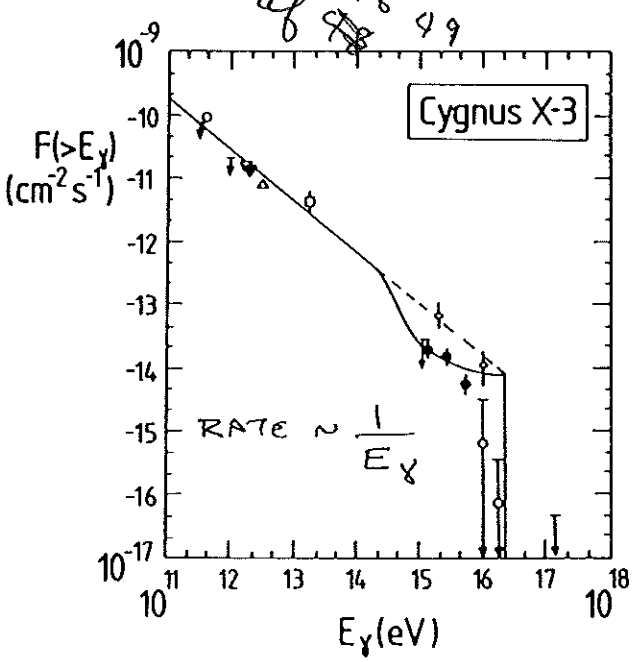

Figure 5.20. γ-ray spectrum from Cygnus X-3 (Rana *et al.* 1984). Best fit spectra with and without attenuation by collisions with microwave background photons are shown by continuous and dashed lines, respectively. Data at $E_\gamma < 10^{14}$ eV are from: ○, Lamb *et al.* (1982); ▽, Stepanian *et al.* (1982); ▼, Danaher *et al.* (1981); △, Mukanov *et al.* (1980); □, Morello *et al.* (1983), and upper limits, Helmeken *et al.* (1979). Data at $E_\gamma > 10^{14}$ eV are from: ◇, Samorski and Stamm (1983*a*); ● and upper limits with circles, Lloyd-Evans *et al.* (1983*a*); upper limits at 10^{15} and 10^{17} eV, Hayashida *et al.* (1981).

IT IS CONTROVERSIAL THAT THE TOTAL γ FLUX FROM A FEW BINARY SYSTEMS IMPLIES CHARGED PRIMARIES SUFFICIENT TO ACCOUNT FOR THE ENTIRE GALACTIC CHARGED COSMIC-RAY SPECTRUM.

COULD THE BINARY X-RAY SOURCES ALSO BE NATURE'S ACCELERATOR, PRODUCING 10^{19}- eV PROTONS - THE COSMIC-RAY PRIMARIES?

PROTONS OF THAT ENERGY CAN REACH THE EARTH ALMOST UNDEFLECTED BY THE GALACTIC MAGNETIC FIELD. CAN POINT SOURCES OF PROTONS BE FOUND?

SOME OF THESE PROTONS WILL INTERACT NEAR THE SOURCE, PRODUCING π^0'S WHICH DECAY TO γ RAYS OF $\sim 10^{19}$ eV ALSO. A CORRELATION BETWEEN SUCH PHOTONS AND PROTONS WOULD BE VERY SUGGESTIVE.

E. THE FLY'S EYE DETECTOR.

ONE OF THE MOST AMBITIOUS PROJECTS UNDER WAY TO EXPLORE (50) THIS IS BASED AROUND THE FLY'S EYE DETECTOR. THIS DEVICE IS PHYSICALLY SIMILAR TO A ČERENKOV SHOWER ARRAY, BUT IS DESIGNED TO DETECT SCINTILLATION OF ATMOSPHERIC NITROGEN. THE SHOWER NEED NOT POINT AT THE DETECTOR, SO THE EVENT RATE IS MUCH HIGHER THAN FOR ČERENKOV DETECTORS.

THE TIME HISTORY OF LIGHT HITTING EACH OF THE 880 ELEMENTS IS RECORDED, SO THE ENTIRE SHOWER DEVELOPMENT CAN BE RECONSTRUCTED. THIS WILL SEPARATE PHOTON FROM PROTON SHOWERS.

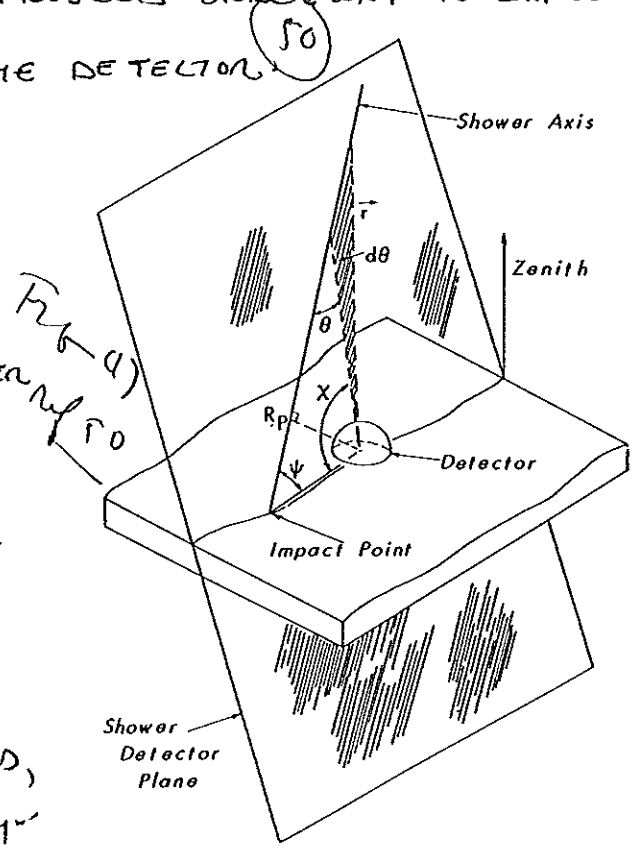

Fig. 5. Geometry of an EAS trajectory as seen by the Fly's Eye. The shower-detector plane contains both the EAS shower and the center of the Fly's Eye detector. It is specified by fits to the spatial pattern of "hit" PMTs which must lie along a great circle on the celestial sphere. The angle ψ and impact parameter R_p are obtained by fits to observation angles χ_i vs time of observation.

TWO EYE'S 3.5 KM APART WILL ALLOW A STEREO RECONSTRUCTION OF THE SHOWER AS WELL.

THE EYE IS TO BE COMPLEMENTED BY A LARGE ARRAY OF SCINTILLATION COUNTERS TO DETECT THE ELECTRON COMPONENT OF EXTENSIVE AIR SHOWERS WHICH STRIKE THE EYE. 1069 DETECTORS IN A 33 x 33 ARRAY WILL COVER 1 Km^2

Fig 48 ref 51

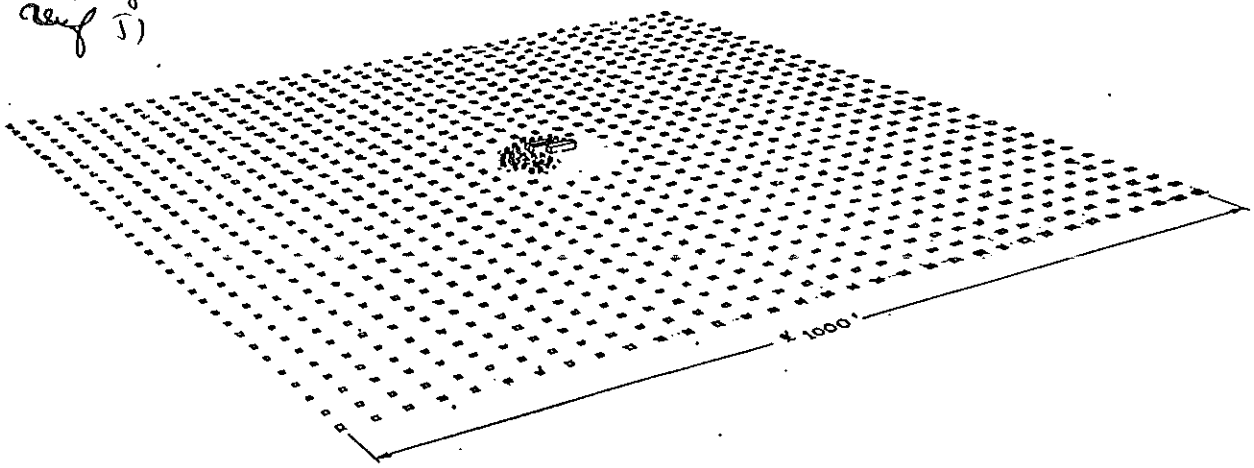

BIRD'S EYE VIEW
CHICAGO AIR SHOWER ARRAY AT THE FLY'S EYE

AN AUXILIARY ARRAY OF UNDER GROUND SCINTILLATORS SAMPLES THE MUON CONTENT OF THE SHOWER TO DISTINGUISH PRIMARY PHOTONS FROM PROTONS. AS IT HAS A 100% DUTY CYCLE THE AIR-SHOWER ARRAY HAS A FLUX SENSITIVITY COMPARABLE TO THE EYE ITSELF.

THE TABLE ON p. 23 SUMMARIZES RELATED DETECTORS UNDER CONSTRUCTION AND IN OPERATION.

PERHAPS THIS NEW GENERATION OF DETECTORS WILL AT LAST ANSWER HESS' 1912 QUESTION AS TO THE ORIGIN OF THE COSMIC RADIATION.

APPENDIX A

In the following tables the present or planned air shower arrays are listed along with their approximate properties. This information was kindly provided by Professor M. Samorski of Kiel University.

Table I

Location		Group	Lat.	Long.	Elev.	Depth gm/cm^2
Moscow	USSR	Moscow	55.7°N	37.4°O	192	1010
Haverah Park	England	Leeds	54.0°N	1.5°W	100	1020
Caucasus	USSR	Moscow	43.5°N	43.0°O	1700	840
Tien Shan	USSR	Moscow/. Sofia	42.5°N	75.0°O	3340	690
Gran Sasso	Italy	Turin	42.5°N	13.6°O	2000	800
Utah	USA	Utah	40.5°N	112.3°W	1460	860
Armenia	USSR	Moscow	40.3°N	44.1°O	3250	695
Mt. Norikura	Japan	Japan/ Collab.	36.0°N	137.5°O	2780	735
Los Alamos	USA	US/Collab.	35.8°N	106.2°W	2110	790
Akeno	Japan	Japan/ Collab.	35.5°N	138.5°O	900	920
La Palma	Germany	Kiel	28.8°N	18.0°W	2200	790
Kolar Gold Field	India	Bombay/ (Tata)	13.0°N	78.3°O	930	920
Ooty	India	Bombay/ (Tata)	11.4°N	76.8°O	2200	790
Chacaltaya(I)	Bolivia	Japan/ Bolivia	16.3°S	68.2°W	5200	530
Chacaltaya(II)	Bolivia	Japan/ Bolivia	16.3°S	68.2°W	5200	530
Adelaide	Australia	Adelaide	35.0°S	138.5°O	100	1020
Utah	USA	this proposal	40.5°N	112.3°W	1460	860

Table II

Experiment	(1)	(2)	(3)	(4)	(5)	(6)
Moscow	7	1 at 1 m^2 6 at 0.5m^2	10^4	3°	10^{15}	1985
Haverah Park	32	1m^2	4×10^4	1°	10^{15}	1986
Caucasus	508	.5m^2	5×10^3	1.2°	3×10^{14}	1984
Tien Shan	115	various sizes	10^4	3°	10^{14}	1974
Gran Sasso	560	.5m^2	10^4-10^5	1°	10^{13}-10^{14}	1988
Utah	36	.1m^2	~10^5	1°	10^{15}	1986
Armenia	-	-	unknown	-	10^{14}	1986
Mt. Norikura	88	1m^2	10^4	1°	10^{14}	?
Los Alamos	72	1m^2	10^4	$\leq$1°	2×10^{14}	1986
Akeno	56	1m^2	10^4	3°	10^{15}	1981
LaPalma	32	1m^2	10^4	1°	10^{14}	1988
Kolar Gold Field	61	1m^2	1.7×10^4	1.5°	10^{15}	1984
Ooty	24	.36-1.44m^2	5×10^3	2°	10^{14}	1984
Chacaltaya(I)	36	1m^2	10^4	1°	2×10^{14}	1986
Chacaltaya(II)	35	31 at .25m^2 4 at 1m^2	3×10^2	3°	2×10^{14}	1986
Adelaide	27	19 at 1m^2 8 at2.25m^2	7×10^4	2.5°	10^{15}	1984
This proposal	1069	1.5m^2	10^5	0.5°	$\leq10^{14}$	1989

(1) Number of detectors
(2) Area of each detector
(3) Effective area of array (m^2)
(4) Angular resolution
(5) Minimum energy (eV)
(6) Start of operation